Crack Propagation Behavior and Toughness of V-Notched Polyethylene Terephthalate Injection Moldings

Bernard Chukwuemeka Ogazi-Onyemaechi, Yew Wei Leong, Hiroyuki Hamada

Advanced Fibro Science, Kyoto Institute of Technology, Sakyo-ku, Kyoto 606-8585, Japan

Received 23 July 2009; accepted 27 September 2009
DOI 10.1002/app.31496
Published online 23 November 2009 in Wiley InterScience (www.interscience.wiley.com).

ABSTRACT: The role of the skin and core regions in controlling the effects of V-notches, on the fracture behavior of PET injection-moldings, was correlated with their tensile and impact properties. Investigations revealed that there were three distinct fracture behaviors: ductile, semiductile, and brittle fracture transitions. The notch sensitivity factor for strength (K_S) in the ductile and semiductile transitions indicates that the fracture strength was not sensitive to $\leq$1.5 mm deep notches, which is considered the skin region. The introduction of core-deep notches (>1.5 mm) resulted in a rapid increase in K_S. On the other hand, the notch sensitivity factor for energy (K_T) shows that the fracture energy was not sensitive at $\leq$0.5 mm deep notches. However, K_T increased drastically when notches >0.5 mm deep were introduced. The development of an anisotropic skin-core structure in injection moldings is well acknowledged. This is revealed in a constant fracture behavior between 0.6 and 1.0 mm deep notches. Notably, there was a drastic change in the fracture pattern from ductile to semiductile at a critical 0.6 mm deep notch. The specimens experienced a mixed fracture behavior at 1.5 mm deep notch, which marks a transitional fracture pattern at the interface between the skin and core regions. Lastly, a constant fracture behavior was observed at notch depths $\geq$1.5 mm. Results show that crack opening, in the samples that had semiductile fracture, was a postnecking phenomenon. Before shear yielding, two shear lines that intersected at 45° were seen to originate from the crack root when a 1.2 kN load was applied. Conversely, crack opening and failure occurred simultaneously in brittle fractures. It is obvious that V-notches provided a gradual transition in fracture behavior from the skin to the core regions, which confirms that the fracture behavior of PET injection moldings can be dependent on the skin and core structure. © 2009 Wiley Periodicals, Inc. J Appl Polym Sci 116: 132–141, 2010

Key words: V-shaped notch; skin; interface; core; fracture behavior; PET injection moldings

INTRODUCTION

Fractures occur in materials when there are preexisting cavities or nucleation of voids due to stressful loading. Such defects in engineering thermoplastic components are stress concentrators[1] that tend to undermine the structural stability of such components during their life span. The resultant effects of cavities, voids, or defects in engineering structures so often can be catastrophic. Catastrophic failure of structures claims heavily in economic and human cost. The study of fracture mechanics, therefore, is meant to investigate the materials' response to fracture under a predetermined crack condition. Understanding the fracture behavior of materials with different sizes of defects helps components designers and engineers to balance between the choice of discarding very expensive defective material and safety requirements of engineering construction. Polyethylene terephthalate (PET) is a semicrystalline thermoplastic material known to be very notch sensitive. The notch sensitivity of PET products had led to many research investigation, which reveals that both virgin (V-PET) and recycled PET (R-PET) products exhibit low fracture resistance in the presence of notch. Takano and Nielsen[2] examined the effect of standard V-notches on polymeric materials including PET by conducting tensile test on dumbbell test bars with single and double edge notches of 1.27 and 3.175 mm deep. Equations (1) and (2) were used to calculate the notch sensitivity factors for fracture strength (k_S) and energy to fracture (k_T), respectively. Results show that if a notch has no effect on the toughness of a polymeric material, the notch sensitivity factor is 1.0, otherwise it is greater than 1.0. Their investigation shows that the values of k_S for PET at 1.27 and 3.175 mm notch depths were 1.02 and 1.26, respectively, whereas k_T at the two notch depths were 7.33 and 11.21. These results, therefore, prove that notches $\geq$1.27 mm are detrimental to PET products as they fracture in a brittle manner.

In recent years, there is much effort to improve the mechanical properties of PET products as demonstrated in the work of Tanrattanakul, et al.[3] They investigated the improvement in toughness of different blends of PET by conducting tensile test on

Correspondence to: B. C. Ogazi-Onyemaechi (emmy_ogazi@yahoo.com).

standard 2.54 mm deep-notched Izod bars at a temperature range of −20 to 55°C. Their work showed that the PET samples blended with unfunctionalized styrene-butadiene-styrene (SEBS) yielded at the crack root, thereby, fracturing in a brittle manner. On the other hand, blending PET with small amounts of functionalized SEBS elastomers was effective in increasing the ductility (toughness) of PET products. The fracture toughness of a material is known to be dependent on its morphological structure and crystallinity.[4,5] Therefore, Stearne and Ward[5] investigated the effect of molecular weight and crystallinity on the notch sensitivity of PET injection moldings. They obtained two samples of varying degrees of crystallinity by varying the sample cooling time in the mold and the mold temperature. They conducted tensile test on the dumbbell samples cut with two notch conditions of 1.91 and 2.79 mm deep. Their investigation revealed that crystallinity affects both the brittle fracture strength and yield behavior of PET injection moldings. They showed that at $\leq$35% crystallinity, there was little influence on the brittle stress, but the yield stress increased. However, at 44% crystallinity, the brittle stress was greatly reduced. Their results also indicate that notched samples had higher yield stress in the cold-drawing region than the un-notched when tested at temperatures above 5°C.

The above reviewed studies investigated only 2.54 mm, and 1.91 and 2.79 mm standard notch depths (ASTM D256) in each case. As injection moldings are known to exhibit anisotropic skin-core morphological behavior, these notches are usually deep enough to penetrate through the skin region. As such, the introduction of standard notches does not provide adequate consideration for the influence of the skin region on the fracture characteristics of the bulk material. Furthermore, in slow crystallizing materials such as PET, the development of a distinct skin-core structure during injection molding is inevitable. PET is known also to be a very notch-sensitive material and would fracture in a very brittle manner upon introduction of notches but remains very tough if un-notched. However, the effect of notch depth on the fracture characteristics is still unclear. Therefore, it is necessary to introduce notches at various depths and examine their effects on the crack propagation behavior of injection molded PET products. If a correlation between fracture characteristics and morphology could be established, the information will be very useful to assist molders in optimizing molding conditions as well as improve the safety and reliability of the moldings.

To understand these effects, V-notches ranging from 0.5–4.5 mm depths were introduced on single edges of dumbbell and Izod impact samples. These depths were chosen so that the notch root was positioned along the skin through the core regions of the moldings. Skin and core regions were determined through polarized optical microscopy. The fracture characteristics of the samples at various notch depths were monitored, during tensile and impact testing, by various optical devices including a CCD camera.

METHODOLOGY

Material and sample preparation

Amorphous grade neat PET (V-PET) pellets (MA2103 LOT 601K; M_w = 23,000) were obtained from UNITIKA, whereas recycled PET (R-PET) flakes were obtained from Yasuda-Sangyo. V-PET pellets were used as received, whereas R-PET flakes were extruded and pelletized before injection molding. The flakes were dried at 120°C for at least 2 h before extrusion by a set of single-screw extruder (SR-Ruder Bambi SRV-P70/62 from Nihon Yuki., Japan). Barrel temperature was set between 255 and 290°C, and screw rotation speed was 50 rpm.

Before injection molding, the V-PET and R-PET pellets were dried for at least 4 h at 130°C, in a PIC-COLO hopper-dryer from Itswa. The fabrication of dumbbell samples was performed with a TOYO PSS TI-30F6 injection-molding machine at a barrel temperature range of 250–270°C. Mold temperature was set at 30°C, while the injection and holding pressures were set at 60 kgf.

Notching and mechanical property characterization

V-notches of 0.5–4.5 mm depths were introduced on dumbbell and Izod impact test pieces with a Tool A-3 Digital Notching Machine (from Toyo Seiki Manufacturing). The notching was performed in stages of 0.5 mm depth to minimize internal deformation of the samples. The angle of the V-notches is in accordance with ASTM D256.

Tensile testing of notched and un-notched dumbbell specimens was performed with an Instron 4466 universal testing machine mounted with 10 kN load cell and set at a crosshead speed of 10 mm/min. At least seven sample pieces were tested for each material and notching condition. As the test progresses, CCD camera was used to monitor the notch tip during crack opening and propagation, while scanning electron microscopy was used to observe the fracture surfaces. Other sets of samples bearing the notch depths of 0.6, 1.5, and 2.0 mm respectively were loaded to intermediate points on the stress–strain curves and stopped. These points include 1.2, 1.4, and 1.6 kN. The samples were carefully unloaded, polished, and observed in polarized optical microscopy to determine the crack behavior at these points. Izod impact testing was conducted with a

TOYOSEIKI Digital Impact Tester machine fitted with a standardized JIS K7110 Hammer bearing impact energy of 2.75 J.

Determination of notch sensitivity factors

Investigations were conducted on the effects of V-notches by analyzing the notch sensitivity factors k_S and k_T at the successive notch depths. This gives an understanding of the effects of notches on the fracture behavior of the materials. If notches have no detrimental effects on the tensile strength and total energy absorbed upon deformation, the notch sensitivity factors for the strength (k_S) and energy (k_T) are equal to 1.0. Conversely, if they have detrimental effects, the notch sensitivity factors are greater than 1.0.[2] In this study, the notch sensitivity factors are determined by the following equations:

$$k_S = \left[\frac{(YS_0) \times [t(w - a_i)]}{(YS_i) \times (tw)}\right] \quad (1)$$

$$k_T = \left[\frac{A_{0\text{ssc}} \times [t(w - a_i)]}{A_{\text{issc}} \times (tw)}\right] \quad (2)$$

where k_S = notch sensitivity factor for yield strength, k_T = notch sensitivity factor for energy. YS_0 and YS_i = yield stress (strength) of un-notched and notched samples, respectively [subscript i is the successive notch depths], t = thickness, w = width, and a = notch depth. $A_{0\text{ssc}}$ and A_{issc} are the areas under the stress–strain curves for un-notched and notched specimens, respectively.[2]

The notch sensitivity factor for yield/fracture strength gives an understanding of how notches affect the strength of materials. On the other hand, the notch sensitivity factor for energy measures the effect of notches on the toughness of the materials.

Measurement of crystallinity in PET

Sample measuring 5.6 mg was extracted from across the middle portion of the cross-section of dumbbell samples. DSC was conducted with DSC Instrument model 2920 MDSC. The sample was heated up to 300°C at 10°C/min and cooled under room air. The enthalpies due to cold crystallization [E_C] and melting [E_M] were measured from the resulting DSC curves. The crystallinity of the materials due to processing [E_P] was then calculated by [$E_P = E_M - E_C$] as shown in Table II.

Birefringence observation of PET Injection-moldings

Birefringence observation was performed on the cross-section of dumbbell samples to gauge the sizes of the skin and core regions. Before polarized-optical-microscopy, a short section of dumbbell specimen was cut and placed in epoxy lamina. One side of the cross-section was polished with a rotational polishing wheel mounted with abrasives of different grain sizes to achieve smooth surfaces. The abrasives were used in stages from large rough grains to smooth finer grains until a smooth surface was achieved. The surface was further made as smooth and clean as possible by the use of alumina cleaner. Thereafter, the first polished side was glued to a clear and clean glass slide with araldite glue to hold it in place and ensure that liquid does not penetrate in-between the glass and sample surface during the polishing of the opposite end of the specimen. It is left to dry. The polishing steps described above were repeated for the opposite view of the cross-section until a thin smooth and translucent view of about 30 μm thickness was achieved. Polarized optical micrographs were taken from the polished specimen through a 3.34 mega pixel Nikon digital camera attached to a 10 X/0.25P magnification optical lens that is mounted on Nikon ECLIPSE E600 Polarizer. The micrographs were joined together by the use of Adobe Photoshop CS software. The resulting composite image panorama was converted to gray mode with Origin 7 J [Rel v7.0265 (B265)] software by OriginLab Corporation; the contours and plots of the frequency and amplitude of their gray values over the entire cross-section were taken and analyzed.

The tensile test samples that were loaded midway to 1.2, 1.4, and 1.6 kN, equally, were observed for fracture initiation. The lateral view of the area containing the notches on the test pieces were cut and placed in epoxy lamina. One side of the lateral view was polished with rotational polishing wheel as described previously in the preceding paragraph. The polished view was glued to a clean and clear glass slide and kept to dry. The polishing steps described above were repeated for the opposite lateral view of the samples until a thin smooth and translucent view of about 30 μm thickness is achieved. Polarized optical micrographs were taken from the polished specimen through a 3.34 mega pixel Nikon digital camera attached to a 10 X/0.25P magnification optical lens that is mounted on Nikon ECLIPSE E600 Polarizer. The micrographs were joined together by the use of Adobe Photoshop CS software and, subsequently, observed for evidence of possible crack opening at the three intermediate load points.

RESULTS AND DISCUSSION

Cross-sectional observation by polarized light microscopy

The polarized optical micrographs of the cross-section of V-PET and R-PET specimens are shown in

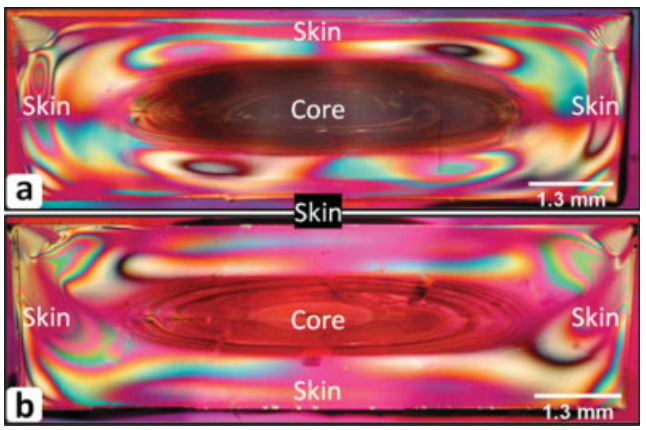

Figure 1 Birefringence observation of the cross-section of dumbbell specimens showing the skin and core structures of a, V-PET and b, R-PET, respectively. [Color figure can be viewed in the online issue, which is available at www.interscience.wiley.com.]

Figure 1(a,b). Distinct skin and core regions could be recognized from the birefringence and contrast of the micrographs. The figures were then converted to grayscale, and subsequently, contour plots defining the intensity of the gray areas were obtained by using Origin 7 J [Rel v7.0265 (B265)] software by OriginLab Corporation, which are depicted in Figure 2(a,b). The contour plots revealed a more complex morphology where the existence of an interface between the skin and the core is clearly visible in both materials.

Derivations from the intensity of the gray areas were used to determine precisely the thickness of the skin and core regions, as shown in Figure 3(a,b). The plots marked with *W* and *X* represent the intensity values of the gray scale in the width and thickness directions of the samples, respectively. The horizontal and vertical cursors on the matrix (gray scale image) were adjusted along the width and thickness directions until well-defined frequency peaks were obtained. The center region in between the two maximum peak intensities [marked by arrows in Figure 3(a,b)] obtained from *W* and *X* plots were taken to be the core width and thickness, respectively. The remaining areas surrounding the core will be regarded as the skin. The thickness values of the skin and core were obtained from the *W* and *X* plots with data points and screen readers provided in the Origin 7 J processing software. These values are presented in Table I. As notches were introduced in the width direction, the thickness of the skin region in this direction is noted to be 1.47 mm on each side of the specimen.

Effect of V-notch depth on tensile properties of PET

Figure 4(a,b) shows the typical stress/strain curves during tensile tests for V-PET and R-PET specimens, respectively. The curves depict the transitions in fracture behavior corresponding to various notch depths. Results indicate that the un-notched samples from both materials maintained high ductility and did not fracture below 300% strain. The introduction of a 0.6 mm deep notch onto the materials, however, resulted in a drastic reduction in the ductility of both materials. This marked a change in the fracture behavior of the materials from ductile to semiductile where shear yielding and tearing at the notch tip was evident with increasing strain. Before shear yielding, there were two lines originating from the crack root at an angle of 45° as observed in Figure 5(a).[6] Crack propagation eventually occurred along one of these lines through which the samples ultimately failed as depicted in Figure 5(b).

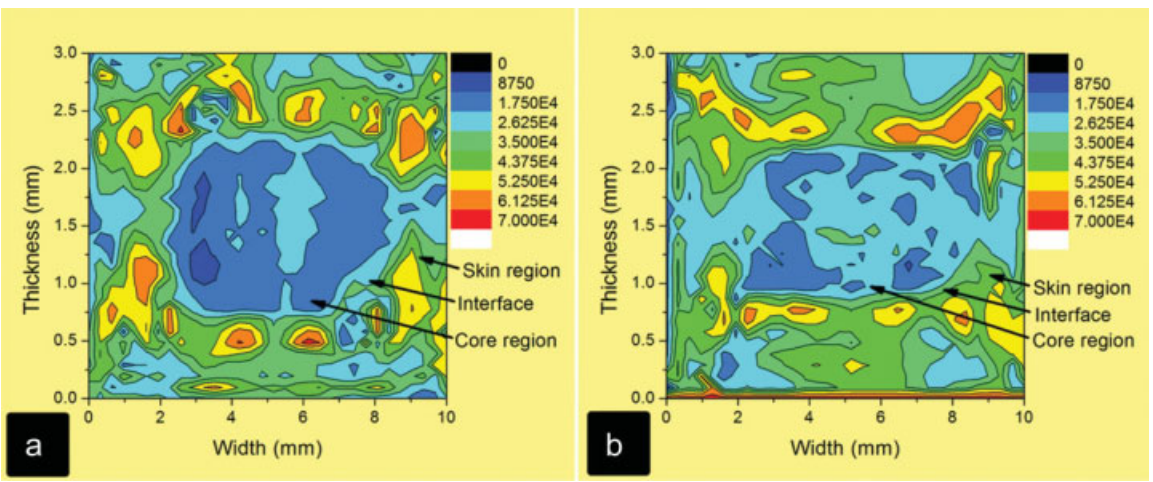

Figure 2 Image contour plots showing the skin, interface, and core regions of a, V-PET and b, R-PET indicated with arrows. [Color figure can be viewed in the online issue, which is available at www.interscience.wiley.com.]

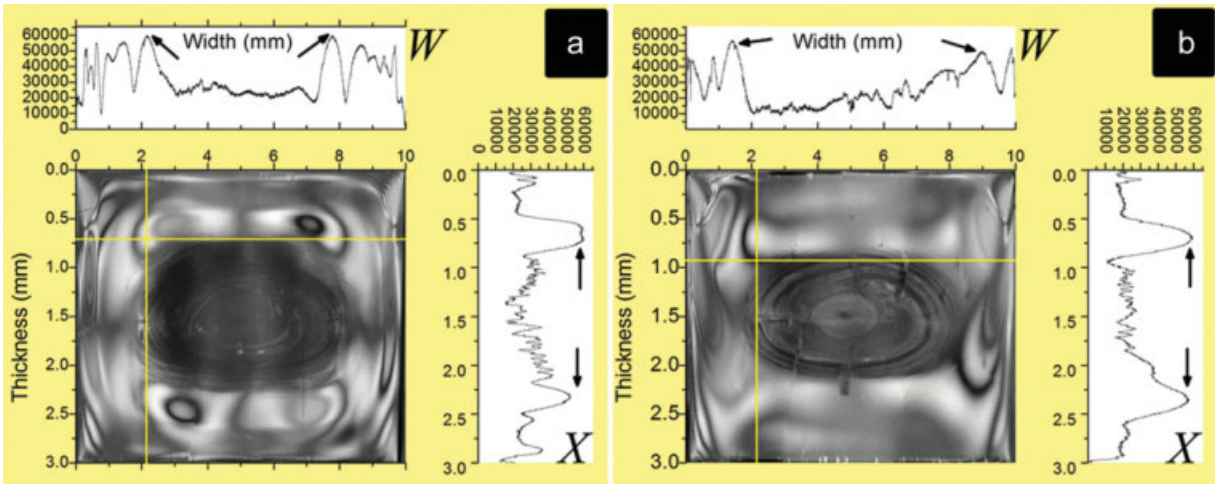

Figure 3 Gray image plots showing the gray values of the skin, interface, and core regions of a, V-PET and b, R-PET [*W* = graph of gray values on the width direction, *X* = graph of gray values on the thickness direction]. [Color figure can be viewed in the online issue, which is available at www.interscience.wiley.com.]

V-PET and R-PET experienced a similar ductile to semiductile transition when notches between 0.6 mm and 1.5 mm deep were introduced, whereas brittle failure was imminent when deeper notches were present (2.0–4.5 mm). It is important to note that the transitions from ductile to semiductile to brittle fracture behaviors were not gradual. A very shallow V-notch, i.e. less than 0.6 mm, would not effectively cause stress concentration; thus, the material remained ductile as in un-notched specimens. When the notch is deep enough to act as a stress concentration point (0.6 mm $\leq a \leq$ 1.5 mm), yielding would occur at the root of the notch. However, the onset of crack propagation would be slow as the notch root was still located within the highly amorphous skin region that is 1.47 mm in thickness, as indicated in Table I. At this notch level, there would be sufficient mobility of the polymeric chain segments for plastic flow to occur at a local (molecular) level from the skin region to the crack tip.[7] With the introduction of notches deeper than 1.5 mm, which would have already penetrated the more crystallized core region, brittle failure was imminent, as there was no further plastic flow from the skin region to the crack tip.

The presence of cracks in materials builds up stress concentration around the defect. It means that the stress acting on the defect is higher than any other part of the material. Increase in the stress results in increase in its intensity until a critical value where the material yields and crack initiates. Therefore, stress concentration factor gives a measure of the sensitivity of materials to cracks. Figure 6 shows the notch sensitivity factors for strength (k_S) at the various notch depths determined by eq. (1). The notch sensitivity factors k_S for the un-notched sample is 1.0, and the notch ranges 0.5–1.0 mm were slightly lower than 1.0. This indicates that the notches had no detrimental effects on the strength of the materials if the notch depths remained $a \leq 1.5$ mm, which is considered the skin region. However, the slight difference between the notch sensitivity factors (k_S) for un-notched sample and 0.5–1.0mm notch depths indicate that these notched samples exhibited higher yield stress than the un-notched specimens. This could be the effect of the stress field at the notch root as it changes from biaxial stress to triaxial,[2] thereby, increasing the materials' resistance to fracture. ASTM D 5045 provides that in the fracture toughness study of a material, the notch depth to width ratio (a/w) would have to be $0.45 \leq a/w \leq 0.55$ so that the material will have minimum resistance to crack propagation. It is obvious that the notches between 0.6 and 1.5 mm fall short of this standard provision. Studies show that the strain rate at the crack tip is greater than the strain rate at any other region on the test piece.[2] Therefore, notches or cracks change the nature of stress field from a biaxial tensile stress to a triaxial stress in the region of the crack. This brings about the twisting of the test

TABLE I
Gray Values from Gray Image plots of the Cross-Sectional View of Dumbbell Samples Showing the Sizes of the Skin, Interphase, and Core layers of V-PET and R-PET

Region of specimen	Width direction (mm)		Thickness direction (mm)	
	V-PET	R-PET	V-PET	R-PET
Skin region	1.47 (×2)	1.47 (×2)	0.65 (×2)	0.65 (×2)
Interphase	0.53 (×2)	0.53 (×2)	0.11 (×2)	0.11 (×2)
Core region	5.98	5.98	1.46	1.46
Total	9.98		2.98	

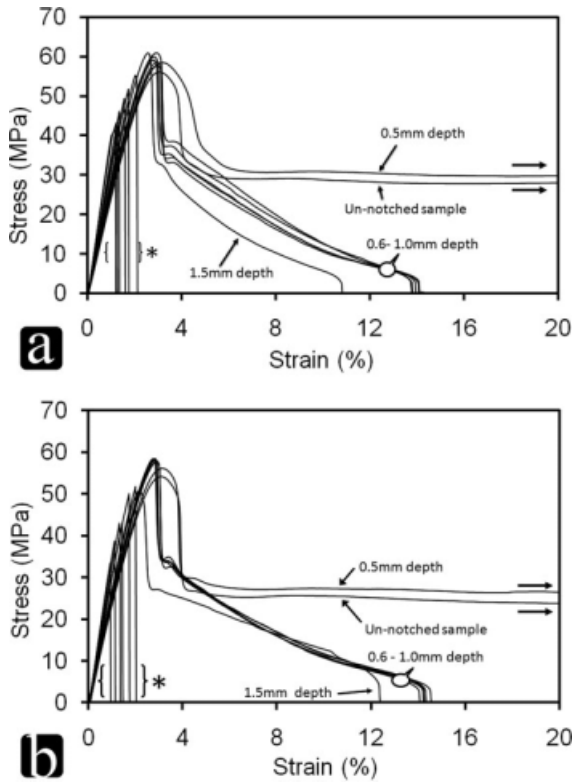

Figure 4 Stress–Strain curves of a, V-PET and b, R-PET showing the effects of V-notch of different depths [{ }* notch depths of 2.0–4.5 mm].

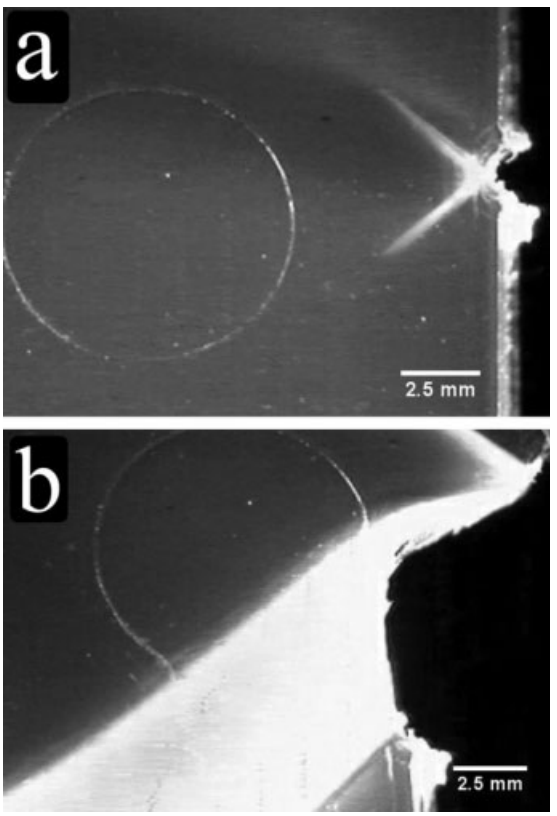

Figure 5 Crack initiation at notch root showing: [a, the development of two lines at an angle of 45° prior to shear banding; b, shear banding and plastic flow due to stress and consequent failure].

sample resulting in a tearing fracture.[2] In addition, results show that V-PET exhibited slightly higher yield stress than R-PET due to higher level of crystallinity, as shown in Table II. It is evident that the yield stress of the materials was not affected by the notch depths of 0.6–1.0 mm.

The notch sensitivity factors for energy (k_T) at the various notch depths calculated from eq. (2) are shown in Figure 7. It is clearly seen that when the notch is $\leq$0.5 mm deep, the k_T value remains at 1.0, which indicates that these notches had no detrimental effect on the materials. However, when the notch depth extends further into the skin region at 0.6–1.00 mm, the k_T value increased to about 6.0. This marks a transition from ductile to semiductile fracture behavior. This shows that while k_S remained stable at $\leq$1.5 mm deep notches, k_T experienced mild detrimental effects.[2] It is clear that both materials (VPET and RPET) experienced similar transition in fracture behavior from ductile to semiductile at notch depths of between 0.6 and 1.5 mm. However, brittle failure was imminent when deeper notches of 2.0 mm and above were introduced. This is evident in the successively higher k_T recorded between 2.0 and 4.5 mm notch depths. As mentioned earlier, three distinct transitions in fracture behavior exist, namely ductile, semiductile, and brittle fracture behaviors. K_S has shown that the materials will remain tough and maintain their structural stability if the notch depth is $\leq$0.5 mm. On the other hand, notches between 0.6 and 1.0 mm deep will be structurally unstable, whereas deeper notches $\geq$1.5 mm will cause catastrophic failure in the materials.

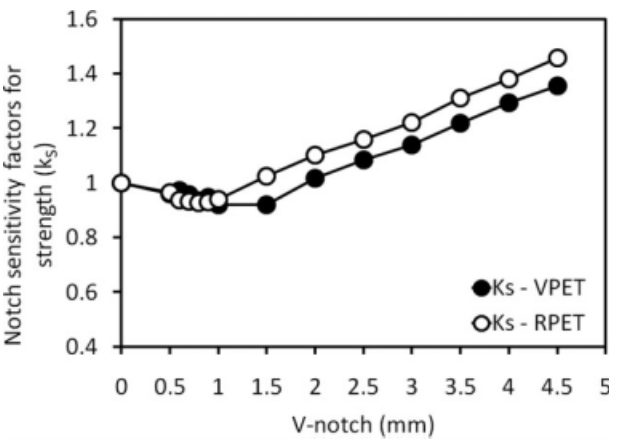

Figure 6 Notch sensitivity factors for strength k_S for the materials at the various notch depths.

TABLE II
The Crystallinity of V-PET and R-PET Injection Moldings

	Cold-crystallization (E_C)		Melting (E_M)		$E_P = (E_M - E_C)$	
Materials	Enthalpy (J/g)	Temp. (°C)	Enthalpy (J/g)	Temp. (°C)	Enthalpy (J/g)	Temp. (°C)
V-PET	19.62	133.72	41.68	257.82	22.06	124.10
R-PET	24.30	129.69	38.09	255.27	13.79	125.58

Fracture modes at intermediate loading points during tensile test

Further investigations were conducted on the three distinct fracture transitions that were identified earlier in Figure 4(a,b) for samples tested at various notch conditions. This was to investigate if crack opening occurred before the necking or failure of specimens introduced with 0.6, 1.5, and 2.0 mm deep notches. Figure 8(a) shows the three loading points 1, 2, and 3 [1.2, 1.4, and 1.6 kN, respectively], on the load-displacement curve for 0.6 mm deep notch samples. The birefringence observation of the samples that were loaded up to points 1, 2, and 3 are shown in Figure 8(b–d). It is seen from Figure 8(b) that two shear lines at angle of 45° had already appeared at the crack root when a 1.2 kN load was applied as indicated by point 1. The loading of a new sample to 1.4 kN, at point 2, resulted in the extension of the two lines toward the opposite end of the sample width as shown in Figure 8(c). The lines continued to extend with higher load (1.6 kN-point 3) until they reach the width end of the samples [Fig. 8(d)] where shear yielding occurred. Figure 8(b–d) show that there was no crack opening in the 0.6 mm deep notch samples before shear yielding; this means that crack opening did not occur in the materials until after shear banding. It is worthy to note that the sample was able to shear band because the 0.6 mm deep notch was still located in the amorphous skin region.

However, the load-displacement curve of 1.5mm deep notch specimens shown in Figure 9(a) shows that the material could sustain only 1.2 kN load before necking and subsequent failure. This means that the material failed below 1.4 kN load when a 1.5 mm deep notch was introduced. Figure 9(b) shows the birefringence of the materials. In the figure, what would have been the two lines originating from the crack root at angle of 45° became straight lines in the direction of the precrack. It is evident that the material yielded at this notch depth, nonetheless brittle failure was imminent. Figure 9(b) clearly shows that the notch was already at the interface between the skin and the core; hence, there was no further plastic flow of the skin toward the crack tip resulting in brittle failure as the crack penetrates the more crystallized core region. This fracture transition marks the onset of brittle failure in the materials when deeper notches were introduced, i.e. the 2.0 mm deep notch samples did not attain 1.2 kN load before brittle fracture.

Tensile fracture surfaces

Figure 10(a–c) represents the fracture surfaces of tensile test (V-PET and R-PET) samples. It is evident that high plastic deformation occurred in the materials at a notch depth of 0.6 mm. This is indicative of ductile failure. It is observed that during crack propagation there was microvoids nucleation around the crack tip (indicated by arrows), which eventually coalesced along the crack path thereby leaving lobe-like fibrils. The microvoid is clearly seen from the images of high magnification camera monitored movie recorded during tensile testing [refer to Fig. (5)]. It is evident also that there was tapering in thickness toward the notch direction as the materials fractured in a semiductile manner from the notch end of the specimen's width to the opposite side [Fig. 10(a)]. This tapering in thickness is caused by a continuous plastic flow[8] from the amorphous skin layer with lower stress concentration toward areas of high stress concentration, such as the notch root,

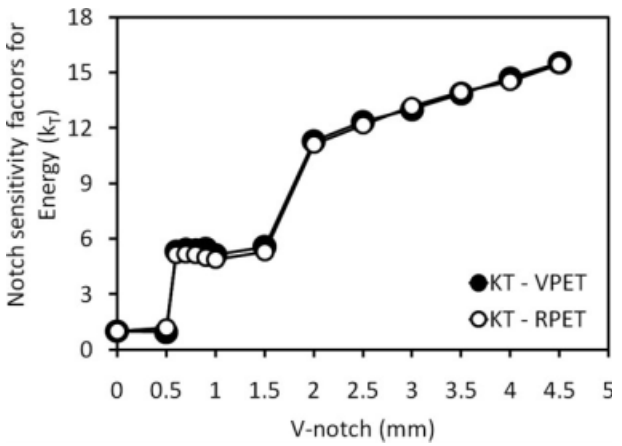

Figure 7 Notch sensitivity factors for energy kT for the materials at the various notch depths.

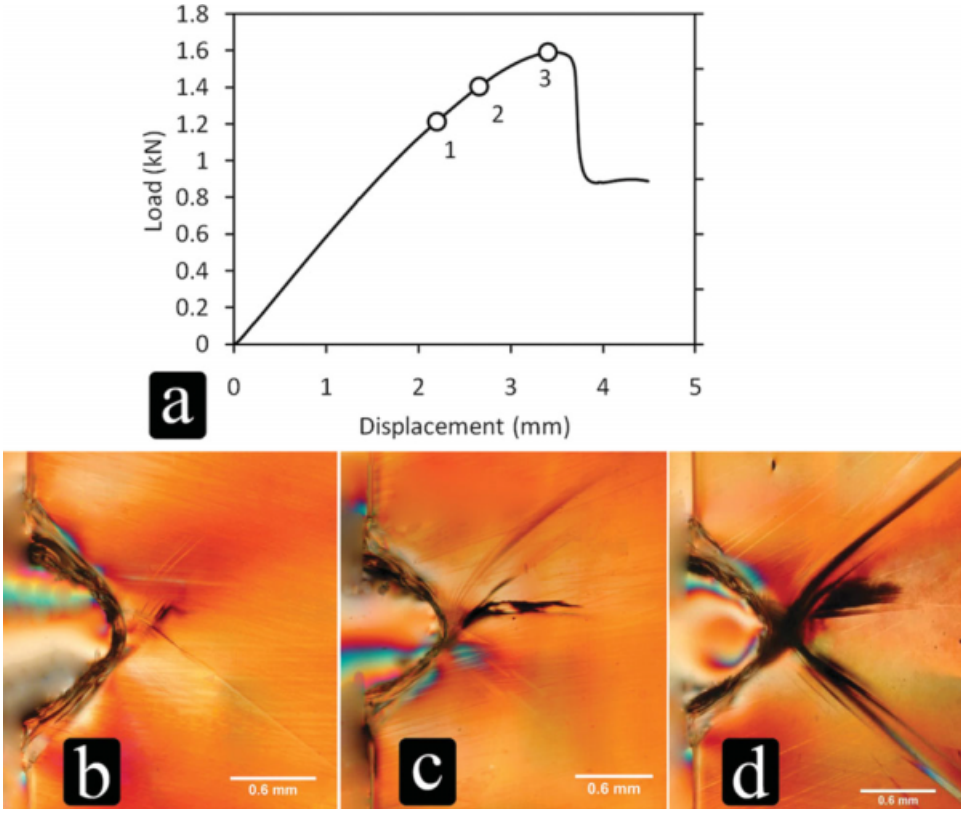

Figure 8 Fracture modes of 0.6 mm deep notch samples at three Intermediate loading points [1, 2, and 3 = 1.2, 1.4 and 1.6 kN, respectively]: a, Load/Displacement curve; b–d, birefringence of samples showing the formation and extension of two families of intersecting slip lines at the respective load points. [Color figure can be viewed in the online issue, which is available at www.interscience.wiley.com.]

which can only occur when the notch does not penetrate through the skin, i.e. notch depth is less than 1.5 mm.

In Figure 10(b), there was a mixed failure (semiductile to brittle fracture behavior).[8] Similar tapering of specimen as seen in Figure 10(a) also occurred in the 1.5 mm deep-notched samples. Nevertheless, it is easy to observe two fracture phases as the notch approaches the interface between the skin and core regions. At the notch root, which contains the terminal part of the skin region, there is significant degree of plasticity. However, as the crack progresses through this interface into the core region, crazing was observed within the core region, as indicated by arrows in Figure 10(b), which lead to semibrittle failure.

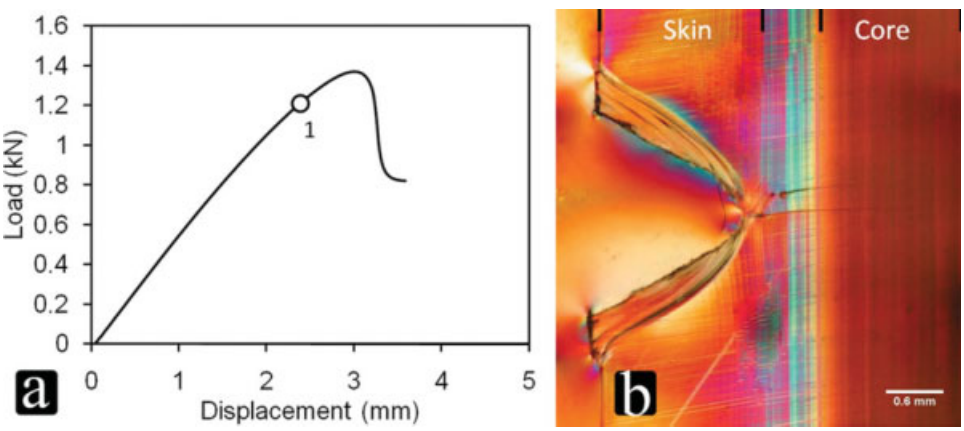

Figure 9 Fracture modes of 1.5 mm deep notch samples at 1.2 kN loading: a, Load/Displacement curve; b, birefringence showing the formation of two straight crack lines when 1.2 kN load was applied. [Color figure can be viewed in the online issue, which is available at www.interscience.wiley.com.]

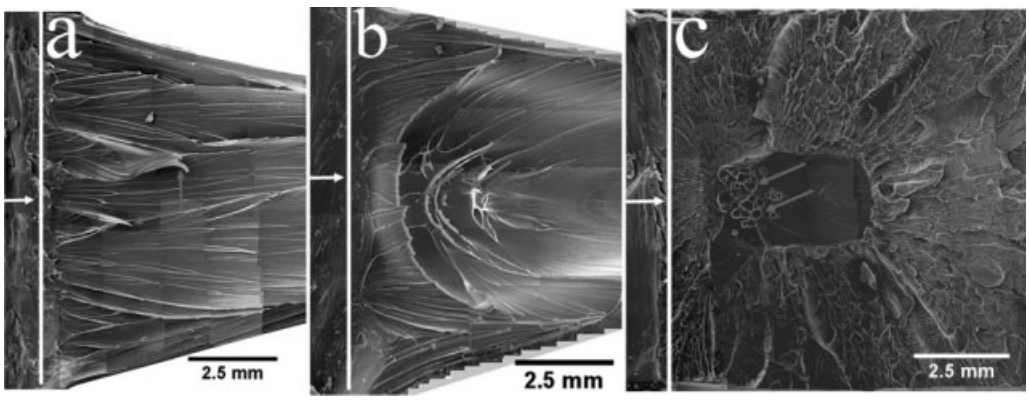

Figure 10 Tensile fracture surfaces showing: a, plastic deformation of the materials at notch depths 0.6 mm; b, plastic to brittle deformation at 1.5 mm deep notch; and c, brittle fracture at 2.0 mm deep notch [arrows indicate notch direction; vertical lines are the end of notches; red lines indicate craze].

Figure 10(c) shows the brittle fracture surface of the materials, when notch depths $\geq$2.0 mm were introduced. Cavities or voids were seen as circular voids at the roots of the notches, but these were unable to coalesce and resist fracture, thereby, forming craze that leads to eventual brittle fracture. It is obvious from Figure 10(c) that there was no tapering of thickness in the specimens when notches have already penetrated the core region. When the notch was core-deep, the plastic flow of the amorphous skin region toward the notch tip was not possible; hence, brittle fracture was imminent.

Effect of V-notches on Izod impact properties of PET

Figure 11 shows that V-PET and R-PET had a gradual loss of strength when impacted upon as the notches deepen. The un-notched and 0.5 mm-notched samples did not fracture upon impact. However, both V-PET and R-PET experienced brittle fracture and recorded impact strengths of about 25 kJ/m^2 when a critical notch depth of 0.6mm was introduced. When subsequent deeper notches of between 0.6 and 1.0mm were introduced, the specimens experienced a gradual but consistent decline in impact resistance. This could be due to the gradual thinning of the amorphous skin region with increasing notch depth, which reduces the effectiveness of the skin in suppressing crack propagation during impact loading. When the notch approaches the boundary between the skin and the core, i.e. the interface 1.5 $\pm$ 0.2 mm, there was a transitional change in the loss of impact strength. Minimum impact resistance in the material was observed when a 2.0 mm deep notch was introduced. Further increments in notch depth resulted in a consistently low impact strength.

The fracture behavior of the materials under impact testing is seen to be different from their behavior under tensile loading. Under impact testing, the impact is very sudden that plastic flow from the skin to the crack tip was not possible; hence,

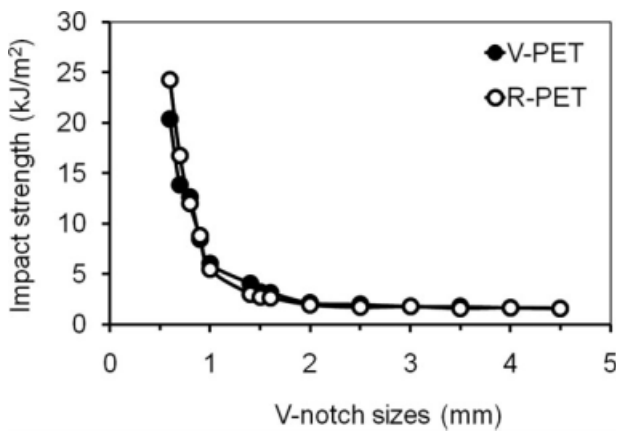

Figure 11 Izod impact strength of V-PET and R-PET showing gradual loss of strength at different V-notch depths.

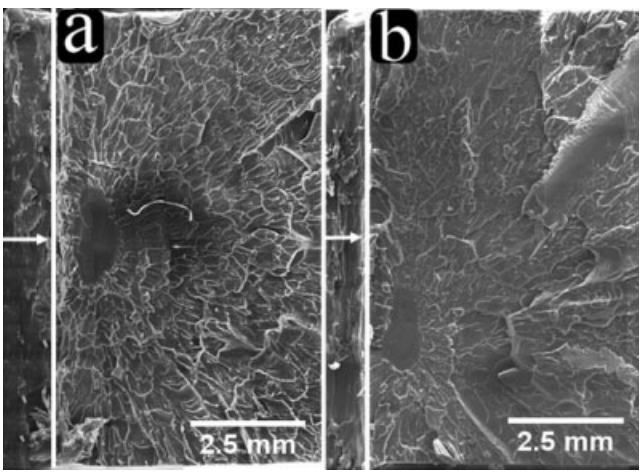

Figure 12 Izod impact fracture surfaces of the materials at various depths of V-notch [arrows indicate notch direction; vertical lines are the end of notch].

they exhibited brittle failure, which was characterized with a gradual and consistent loss of impact strength. However, under tensile loading three distinct fracture behaviors were revealed at different notch depths. This is because while the notches remain at the amorphous skin regions, the molecular chains can slide past one another and realign thereby causing plastic flow[9] toward the crack tip.

Izod impact fracture surfaces

Figure 12(a,b) represents the impact fracture surfaces of VPET and RPET at the various notch depths. The micrographs show similar brittle fracture even as the notches extend deeper into the core region. The circular-shaped craze at the crack root indicates sudden disruption of voids nucleation and coalescence due to impact. It can be concluded that due to sudden impact on the materials, no plastic flow from the skin region toward the stress concentration region was possible.

CONCLUSIONS

This investigation has revealed that the fracture behavior of PET injection moldings responded in transitional phases from the skin through the interphase to the core regions of the samples. Thus, three distinct fracture transitions were clearly observed from the results indicating that the skin and core morphology play significant role in the fracture behavior of PET injection molded components. The notch sensitivity factor (k_S) shows that the fracture strength of the materials will drop drastically if the notch is deeper than 1.0 mm. On the other hand, k_T indicates that notches deeper than 0.5 mm have detrimental effects on the toughness of the materials. Tensile loading provided a transitional fracture behavior from ductile, semiductile to brittle failure of the materials while impact testing resulted in their brittle failure and gradual loss of impact strength. By loading the specimens to intermediate points on the load-displacement curves, it has been shown that crack opening did not occur in the specimens before yielding. Therefore, it could be concluded that crack opening was a postnecking phenomenon in the specimens that failed in a semiductile manner.

References

1. Broek, D. The Practical Use of Fracture Mechanics; Kluwer Academic Publishers: Boston, 1989; p 23.
2. Takano, M.; Nielsen, L. E. J Appl Polym Sci 1976, 20, 2193.
3. Tanrattanakul, V.; Perkins, W. G.; Massey, F. L.; Moet, A.; Hiltner, A.; Baer, E. J Mater Sci 1997, 32, 4749.
4. Kuriyama, T.; Narisawa, I.; Shiina, F.; Kotaki, M. J Vinyl Additive Technol 1998, 4, 164.
5. Stearne, J. M.; Ward, I. M. J Mater Sci 1969, 4, 1088.
6. Ma, M.; Vijayan, K.; Hiltner, A.; Baer, E. J Mater Sci 1989, 24, 2687.
7. Perkins, W. G. Polym Eng Sci 1999, 39, 12.
8. Mills, N. J.; Walker, N. J Mater Sci 1980, 15, 1832.
9. Askeland, D. R.; Phule, P. P. The Science and Engineering of Materials, 4th ed.; Brooks/Cole: USA, 2003; p 669–719.